INCREASING PRODUCTION IN FRACTURED WELLS BY OPTIMIZING WELL COMPLETION PARAMETERS

A Thesis

by

ADITYA RAIZADA

Submitted to the Graduate and Professional School of
Texas A&M University
in partial fulfillment of the requirements for the degree of

MASTER OF SCIENCE

Chair of Committee,	I. Yucel Akkutlu
Co-Chair of Committee,	Siddharth Misra
Committee Member,	Mukul R. Bhatia
Head of Department,	Jeff Spath

December 2021

Major Subject: Petroleum Engineering

ABSTRACT

Unconventional oil and gas reservoirs have low recovery rates and to increase productivity, hydraulic fracturing is used. Hydraulic fracturing allows increased flow of oil and gas to the well. The extended production from these reservoirs and the economic value of the well is controlled by certain qualities of the reservoir and the hydraulic fractures. A sensitivity analysis allows us to understand how various petrophysical and completion factors affect cumulative production from these fractures. By understanding which factors affect production, we can optimize completions to enhance productivity further. The simulation model used for this study is a single fracture well. A compositional equation of state (multi-component multi-phase) fluid transport reservoir simulator is used. The reservoir model considers the matrix consisting of organic and inorganic components, the fracture is imbedded into this matrix as a discreet feature describing a discontinuity. The matrix porosity is made of organic nanopores and inorganic stress-dependent cracks. The experimentation on the sensitivity is split into two phases, where phase 1 is a 15 variable fractional factorial design of experiment model with a resolution 4 and phase 2 is a refined experiment using the top 10 variables from the 1st phase based on Central Composite Design of experiment. The cumulative production was noted after 1 and 3 years of production. From the results, it was found that the maximum confining stress needed to close the inorganic microcracks completely, the parameter indicating the resistance of microcracks to close, and the fracture geometry (more precisely the fracture half-length) were the most influential. These effects amplify over time during the

production. Operationally, the bottom hole pressure is identified the most important wellbore condition with potential to affect the cumulative production.

DEDICATION

This thesis is dedicated to my parents, my family, my friends, my professors, and all others who have contributed to my success. Each of you have made a special impact which has nurtured and molded me into the person I am.

ACKNOWLEDGEMENTS

I would like to thank my committee chair, Dr. Akkutlu, and my committee members, Dr. Misra and Dr. Bhatia, for their guidance and support throughout the course of this research.

Special thanks to Dr. Seunghwan Baek for co-supervising my work and helping me with running the simulations smoothly.

Special thanks to Dr. Bryan Maggard for providing me with a Graduate Teaching Assistantship and guiding me with additional resources in computer programming.

Thanks also go to my friends and colleagues and the department faculty and staff for making my time at Texas A&M University a great experience.

Finally, thanks to my mother and father for their encouragement and love.

CONTRIBUTORS AND FUNDING SOURCES

Contributors

This work was supervised by a thesis committee consisting of Professor Dr. Akkutlu and Dr. Misra of the Department of Petroleum Engineering and Professor Dr. Bhatia of the Department of Geology and Geophysics.

All other work conducted for the thesis was completed by the student independently.

Funding Sources

Graduate study was supported by a fellowship from Texas A&M University, GPA based scholarships from the Department of Petroleum Engineering and a Graduate Teaching Assistantship from the Department of Petroleum Engineering.

NOMENCLATURE

DOE	Design of Experiments
OFAT	One-Factor at a Time
T	Time
USGS	United States Geological Survey
nm	Nanometer
nD	Nano-Darcy
HC	Hydrocarbon
CCD	Central Composite Design
LSE	Least Squares Estimation

TABLE OF CONTENTS

Page

LIST OF FIGURES

Page

LIST OF TABLES

Page

1. INTRODUCTION

1.1. The World of Shale

The United States of America became independent in 1776, however, the country's energy independence came only in the early 2010's. This revolution was led by a rock known as shale. Shale rocks have been around forever but were always looked at as being the source rock for conventional reservoirs without any economic value as a resource. This changed with advances in technology and the oil industry never looked back. The source rock had become the reservoir using a new technique called hydraulic fracturing (Hughes 2013). According to the USGS, "Hydraulic fracturing is the process of injecting water, sand, and chemicals under high pressure into a low permeability bedrock formation". This well development process single handedly changed how people perceived the oil and gas industry and ushered in a new era of prosperity for millions of Americans.

Hydraulic fracturing helps create a complex network of fractures in an otherwise low permeability formation (Holditch 2007). These fractures are interconnected with the well and facilitate the flow of hydrocarbons and increase production. Even still, the recovery factor from these shale oil and gas wells is very low. The average recovery factor for a shale oil well ranges from %10 to %20 (Gherabati, Hammes et al. 2018). This has been a cause of concern for the petroleum engineers since it is much lower than that of the conventional reservoirs. To understand the recovery from unconventional resources one needs to study production as a function of various hydraulic fracture and reservoir matrix parameters and consider their impact on the short and long-term production trends.

To understand why shale wells, have such low recovery factors, we need to dig deeper and discuss the mechanisms of fluid storage and transport within the shale rock matrix.

1.2. Shale Matrix Structure

The shale rock matrix has been characterized by a few different researchers. They have come up with the idea that the matrix is comprised of three different continua namely the inorganic component of the matrix, the organic component of the matrix, and the fractures embedded into the matrix. The inorganic material makes up most of the matrix body, consists of materials such as quartz, feldspars, carbonate, dolomite, clays, pyrite. While the organic matrix, consisting of the kerogen appears as the dispersed solid phase within the inorganic matrix. In certain source rock, in addition to kerogen, the matrix may include bitumen either in the solid or liquid form. Kerogen and solid bitumen maintain their own network of pores, which are typically small (< 1micrometer scale). The natural fractures and micro-cracks improve accessibility to these small pores.

An example showing the organic pores including the network of small pores and capillaries can be seen in the figure 1 below obtained using a focused ion beam scanning electron microscope (SEM) for a Barnett shale sample (Ambrose, Hartman et al. 2012).

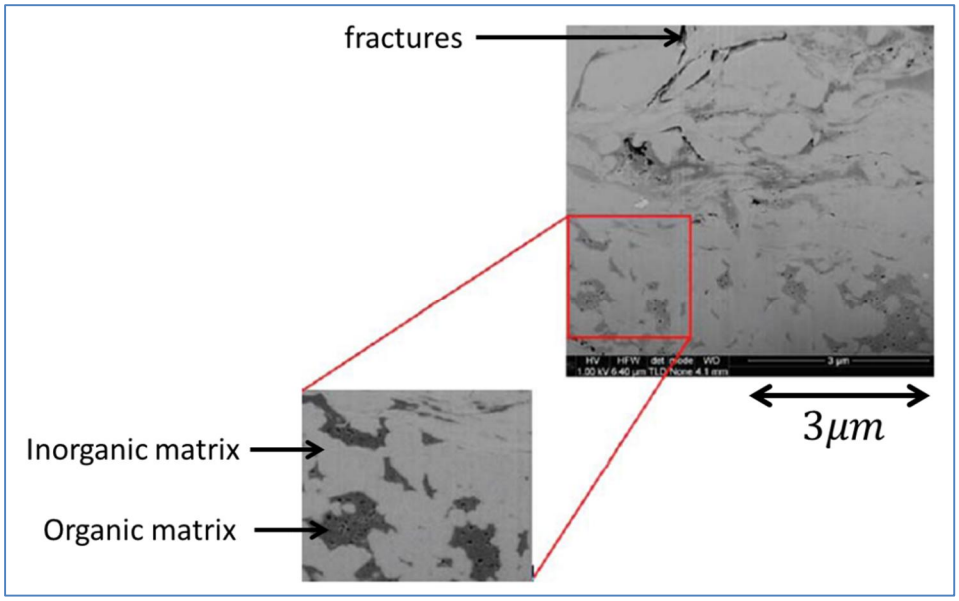

Figure 1: Dispersion of organic matter within the matrix

1.3. Gas Storage in Shales

In shale gas reservoirs, the gas can be stored in a variety of different forms ranging from free gas within the matrix, or as adsorbed gas found on the surfaces of the matrix pore network (Guo, Hu et al. 2017). The free gas storage in shales depends on the pore volume, while the adsorbed gas storage is dependent on the surface area of the pores in the shale (Tang, Jiang et al. 2016).

1.4. Stress-Dependent Permeability

The permeability of the shale matrix generally varies with the effective stress. This phenomenon was addressed by experimental tests, which indicated that the shale matrix permeability is stress sensitive (Akkutlu and Fathi 2012). There are several models developed for stress-dependent permeability in shale, however for my research I used the model introduced by Gangi as it considers micro-cracks as the major flow path of the

unconventional rocks (Gangi 1978). This is important as shales tend to be brittle and inherently rich in micro-cracks.

The "bed of nails" concept introduced by Gangi assumes the distribution of shape-height is a power law function, essentially meaning that the various shapes of the crack including conical, hemispherical, etc. could be treated alike (Gangi 1978).

The model equation is shown below:

$$k_a = k_0\left(1 - \left(\frac{\left(P_{conf} - \alpha P\right)}{P_1}\right)^m\right)^3$$

Here, k_0 is the permeability of the inorganic matrix and P_1 is the maximum stress when the crack closes completely. The value of **m** is dependent on the shape of the crack and the numerator defines the effective stress. This phenomenon has been described in the figure 2 below.

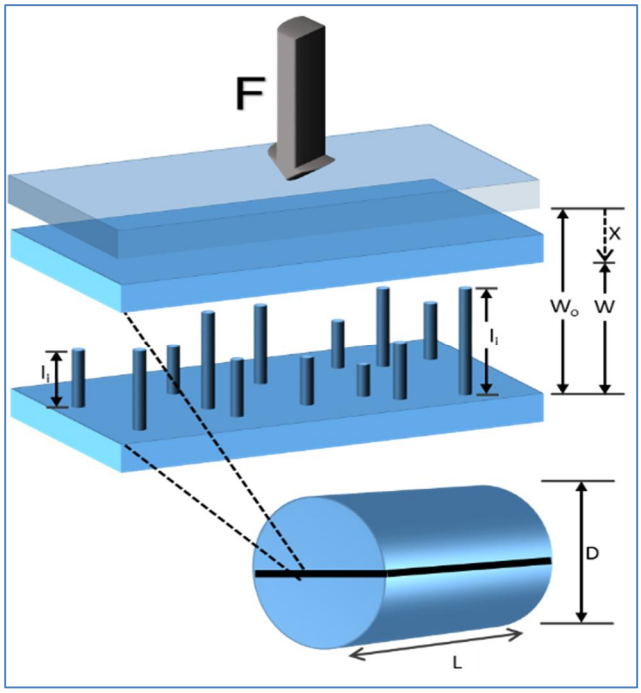

Figure 2: Gangi's Bed of Nails for modeling permeability of fractures. This model is applied as permeability model for brittle shale samples.

1.5. Shale Gas Transport Mechanism

In shales with lower formation permeability as in the order of 1 nD, it was found that molecular diffusion has a significant effect on gas transport (Akkutlu and Fathi 2012). A mathematical model was introduced governing multiscale transport in organic-rich shale which takes into consideration the dual-porosity continua of organic and inorganic matrices and including the molecular and surface diffusion effects (Akkutlu and Fathi 2012). During experimentation, flow regimes changed from a parabolic velocity profile to one of uniform velocity for gas flow in organic capillaries with sizes below 100 nm (Akkutlu and Fathi 2012).

A new permeability model describing shale gas transport with adsorption and diffusion in the organic round pores and diffusion and convection in the micro cracks was introduced (Wasaki and Akkutlu 2015). Shown below is the equation based on the convective-diffusive-adsorptive mass flux for apparent permeability representing the overall gas transport:

$$\boldsymbol{k_{gas}} = \mathbf{k_m} + \boldsymbol{\mu_g c_g D} + \boldsymbol{\mu_g} \frac{\boldsymbol{V_{sL} \rho_{grain} B_g}}{\boldsymbol{\varepsilon_{ks}}} \frac{\boldsymbol{P_L}}{(\boldsymbol{P} + \boldsymbol{P_L})^2} \boldsymbol{D_s}$$

Here, $\mathbf{k_m}$ is the stress-dependent permeability of the shale, $\boldsymbol{\mu_g c_g D}$ is the free gas pore diffusion term and the last term is the adsorbed phase transport in the organic pores. $\boldsymbol{\varepsilon_{ks}}$ considers the organic volume over the total volume, while $\boldsymbol{V_{sL}}$ $\boldsymbol{and}$ $\boldsymbol{P_L}$ are the Langmuir parameter for the adsorbed gas. The diffusion coefficients $\boldsymbol{D}$ (free gas) and $\boldsymbol{D_s}$ (adsorbed gas) are related to the composition making up the gas mixture in the kerogen nanopores.

For binary mixtures, the Maxwell-Stefan diffusion model is one which is used commonly. The advective-diffusive transport in organic-rich shales with multiple HC components was studied with consideration of its pressure-dependence (Olorode, Akkutlu et al. 2017). For a chemical species such as methane, the Maxwell-Stefan diffusion model equation is introduced below in terms of diffusive flux, J.

$$\boldsymbol{J} = -\boldsymbol{c}\, \boldsymbol{\mathcal{B}}^{-1} \boldsymbol{\Gamma} \boldsymbol{\nabla y_i}$$

Here, $\mathbf{c}$ is the concentration, $\boldsymbol{\mathcal{B}}$ is the drag matrix, $\boldsymbol{\Gamma}$ is the thermodynamic factor and $\boldsymbol{y_i}$ is the mole fraction of the gas.

It has been studied that the fluid composition in the reservoir conditions at initial conditions is not the same as the fluid produced at the surface due to adsorption and Nano-confinement effects (Akkutlu, Baek et al. 2017, Bui and Akkutlu 2017). It was further studied that with a decreasing pore size, the apparent molecular weight of the hydrocarbon mixture gets heavier due to nano-confinement effects (Bui and Akkutlu 2017).

To evaluate hydrocarbon volumes in place more accurately, a new concept of fluid redistribution based on molecular simulation of fluids under confinement was introduced (Bui and Akkutlu 2017). This concept investigated the distribution of hydrocarbon mixtures in organic nanopores. From the study, it was concluded that pore size, pressure and temperature affect the composition of these hydrocarbon mixtures (Bui and Akkutlu 2017). This concept helps in providing us with a better idea of the composition of the hydrocarbon fluids initially in place based on measured pore size distribution in the formation.

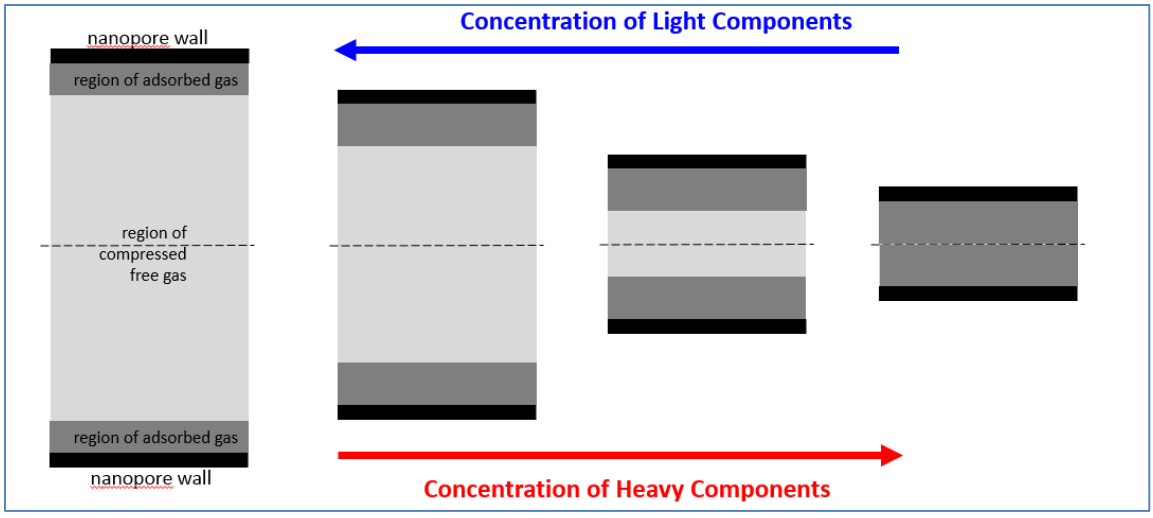

Figure 3: Nanoconfinement Effect

The redistribution partitions the hydrocarbon mixtures into 3 main categories. The smallest organic nanopores, which are just a few nanometers in diameter, contain trapped hydrocarbons, the larger organic nanopores contain the producible hydrocarbons and the bulk hydrocarbons are stored in the large organic or inorganic pores. In this concept, two pore-size cut-off sizes are introduced. The first being the large pore threshold, **ε**, above which the hydrocarbon fluid acts as a bulk phase with its own bulk phase composition and the second being the trapped hydrocarbon cut-off, below which hydrocarbons recovery is significantly more difficult due to nano-scale confinement effect (Bui and Akkutlu 2017). This has been shown in the figure 4 below:

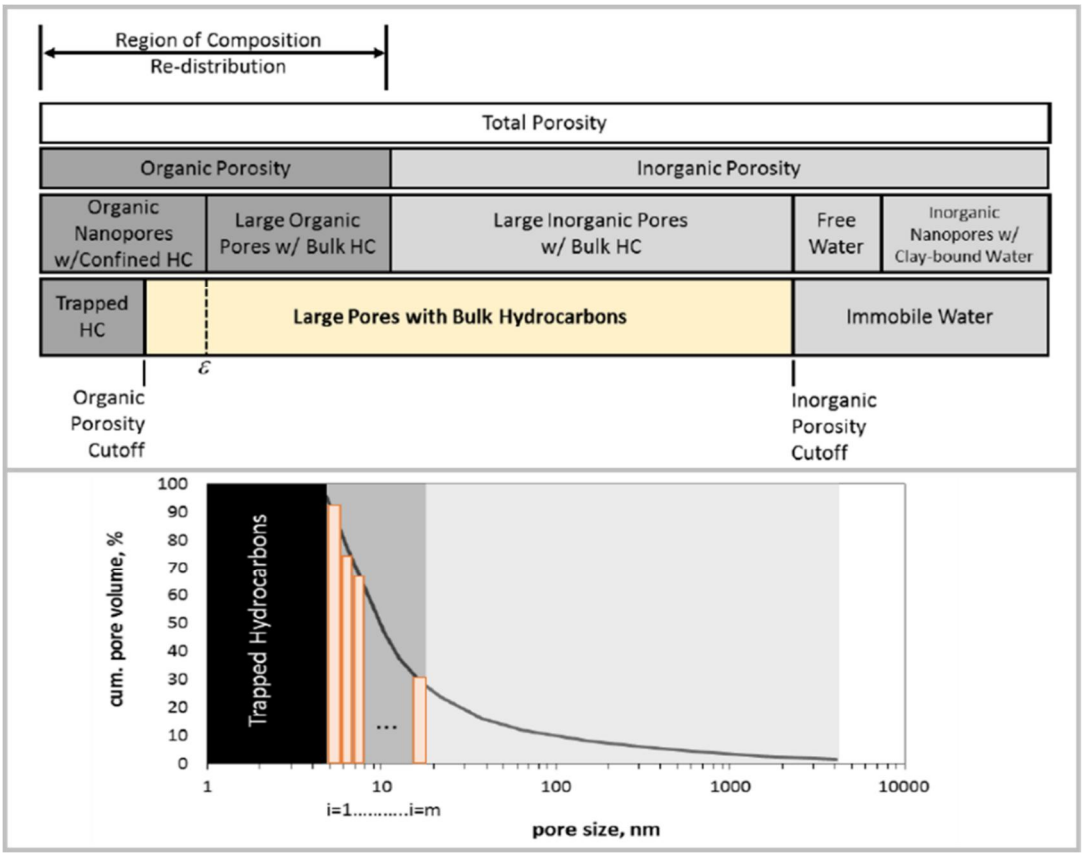

Figure 4: Hydrocarbon distribution partition (Akkutlu, Baek et al. 2017)

1.6. The problem

The dynamics of production from shale oil/gas reservoirs are the least understood ones and most difficult to predict. These reservoirs have a relatively low recovery factor. It is highly practical and economically important that we understand what factors affect the oil and gas production from shale wells. Therefore, I have conducted my studies using a method called design of experiments. This method has helped me perform a sensitivity analysis to find out what are the most important factors for oil production. This study will help us to optimize the well completion parameters and hopefully increase oil production by giving us fresh insight. The analysis takes into consideration the geo-mechanical deformation of the matrix and the hydraulic fractures, using an in-house compositional reservoir simulator that couples geomechanics: NaSh. The screening for the variables will be based on the estimated weighting factor for each variable and their interactions with one another. I will be measuring the changes in the variable sensitivities after 1 and 3 years of cumulative gas production and understand the relationship of the weighting factors over time. I will apply two methods and compare: (1) fractional factorial design method, and (2) central composite design method.

1.7. Target Goal

The main aim of this research is to find the reservoir (fracture + matrix) parameters which have the greatest effect on cumulative gas production during for an unconventional well. This will help us understand which parameters are needed to be optimized to optimize the production system and achieve the highest recovery from shale oil wells.

1.8. Literature Survey

Design of experiments has been used for a variety of applications in the oil and gas industry. More recently it has been implemented for designing simulation runs to understand and characterize the behavior of various systems (Gurav, Dandekar et al. 2019). The applications seen range from optimizing well pattern to that of evaluating petrophysical properties. These applications have generally been utilized in response to a cost measure or oil production over time.

In 1993, a hydraulic fracture design was optimized using a three-dimensional hydraulic fracturing model in conjunction with a fractured reservoir production model (Hareland, Rampersad et al. 1993). The NPV was the response for fracture length and fracturing fluid pump rate. The method was accurately able to predict the net revenue and a relation between the NPV and fracture size was seen. However, increased fracture sizes led to higher costs as well (Hareland, Rampersad et al. 1993).

In 1999, high permeability fracture modelling was able to give an insight into the optimum width for each fracture length by optimizing the expected well performance (Aggour and Economides 1999). The paper suggests that the degree of damage is secondary if the fracturing fluid invasion is minimized. Concluding that severe permeability impairments can be tolerated if leak-off penetration is small (Aggour and Economides 1999).

In 2008, design of experiments was used for history matching of field production data to compute estimated reserves while minimizing the simulation effort (Gupta, Collinson et al. 2008). The authors have presented a four-stage process for history

matching using the design of experiments framework, starting with identifying the uncertain parameters and the history matching parameters. This was followed by design generation. The third step specified models and the response surface was calculated. Finally, the history matching parameters were predicted and goodness of each model was measured. This methodology presented quantifies the probability for each scenario based on history matching parameters and is fast and efficient from trial and error (Gupta, Collinson et al. 2008).

In 2014, design of experiments was used to evaluate the economics for an unconventional resource play. A D-optimal design table has been used to evaluate the impact of various parameters to the project economic measures (Chidi, Xie et al. 2014). An interesting result showed that early production metrics might be affected by drilling and completion times however other factors have a greater impact on net present value (Chidi, Xie et al. 2014).

In 2019, design of experiments was utilized to design simulation runs using parameters such as well type, horizontal well length, well pattern geometry to calculate oil recovery and estimating a well cost for each simulation case (Gurav, Dandekar et al. 2019). The mathematical model used maximized oil recovery and minimized well cost based on Response Surface Methodology. This helped in achieving the optimum combinations of variables in turn to ensure optimum oil recovery and provide insights into developing fields more efficiently (Gurav, Dandekar et al. 2019).

In 2020, design of experiment was used to estimate the oil initially in place (OIIP) by understanding the effects of the petrophysical factors on OIIP (Essien and Akpabio

2020). Monte Carlo simulations were run, and design of experiments was applied using MS Excel and Minitab software and presented in the form of sensitivity indices and tornado plots. Using design of experiments, the authors concluded that porosity has the highest effect on OIIP, followed by oil saturation and pay thickness (Essien and Akpabio 2020).

In 2020, design of experiments was performed for the basis of analyzing hydraulic fracturing of gas wells. The study looked into the influence of hydraulic fracturing parameters on well productivity optimizing well production while minimizing cost (Baioco, Jacob et al. 2020). Various properties such as proppant properties, fracture fluid properties, formation properties, well properties and cost properties have been taken into consideration. The sampling for the data has been performed using a Latin hypercube followed by application of design of Experiments (Baioco, Jacob et al. 2020).

2. DESIGN OF EXPERIMENTS

2.1. What is Design of Experiment?

According to the American Society for Quality, design of experiment (DOE) is a branch of applied statistics that deals with planning, conducting, analyzing, and interpreting controlled tests to evaluate the factors that control the value of a parameter.

The aim of DOE is to identify the set of process factors being most relevant to the process performance and to determine the optimal factor levels to maximize performance providing a powerful and cost-effective method for understanding and optimizing processes (Freiesleben, Keim et al. 2020)

DOE has originated from the work of R. A. Fisher in the early 20th Century. Mr. Fisher was able to demonstrate that before trying an experiment, it was important to consider the design and execution of the experiment. He came up with 3 important principles for conducting experiments (Fisher 1936):

- Replication

  In real life, experiments should be repeated with different experimental units to estimate the experimental error. The experimental unit is the physical entity assigned at random to a treatment.

- Randomization

  The order in which the responses are measured should be randomized to generate an unwanted systematic effect.

- Blocking

  To eliminate unwanted, block to block variation, the experiments are arranged in blocks grouped of homogenous experimental units. A block is a combination of experimental treatments such that any effects on the experimental results due to a known change in operators, machines, etc. become concentrated.

As more experiments are performed, more data is generated, which helps us to characterize the system better. However, running these experiments becomes expensive over time.

2.2. Why the Design of Experiments?

There are multiple methods for initiating experiments and applying sensitivity analysis such as Machine Learning and OFAT.

OFAT stands for One Factor at a Time, commonly used in Engineering. OFAT is applied to find an optimum setting of a variable by continuous change. However, the advantage of DOE over OFAT is that one can characterize not only the main effects but also the interaction effects between the variables (Wahid and Nadir 2013).

Machine Learning is a methodological approach to solve complicated optimizations problems based on abundant data. Both DOE and Machine Learning are concerned with data analysis and application of statistics. DOE is decidedly a human-centered methodology where the engineer applies his knowledge to select the factors to be examined, sets the level values for the factors, and conducts the experiments. However,

Machine Learning is nonhuman and automatically detects patterns in data (Freiesleben, Keim et al. 2020)

2.3. Main Effects

These are the effects caused by the variables individually on the response variable and are generally the more important than the interaction effects. Any changes in the values of the variables are called main effects to the experiment (Fisher 1936).

2.4. Interaction Effects

Many important phenomena depend on the interaction effects of various variables, not only on the operation of one. An interaction effect is the simultaneous effect of two or more independent variables on at least one dependent variable in which their joint effect is significantly greater (or significantly less) than the sum of the parts (Hicks 1964).

2.5. Factorial Design

A factorial design refers to exploring all possible combination of the factors and their levels. The advantage of using a factorial design is that they can estimate the interaction effects while not missing the optimal setting. Different classes of problems such as Nominal-The-Better (NTB), Larger-The-Better (LTB) and Smaller-The-Better (STB) have different procedures to obtain optimize results using factorial design. Through our experimentation, our aim has been to maximize the shale well gas production, therefore modelling a Larger-The-Better problem.

The procedure for an LTB problem is:

- Select the levels of factors to maximize the target variable

- Select the levels of the factors that are not used in the 1st step to minimize the target variable.

Let us take an example of a 2-level, 2-factor full factorial design. Here, we are going to represent the low factor value with a '-' and the high factor value with a '+'. The low factor value is a minimum value at which we would like to evaluate the relationship of the factor to the response, while the high factor value is the maximum. Coding the variable according to the factors, we attain a level '-1' and '+1'. So, to calculate the mileage of a car, we need to know the amount of gas it uses, and we need to know the time we drove it for. We have taken 4 points, which can be seen in Figure 6, with a different level combination at each point.

In Figure 5, the low factor value for gas is 1 Gallon and high factor value is 5 Gallons. The low factor value for time is 30 minutes, while the high factor value is 1 hour. Our response variable is the mileage. The inference we are trying to draw from this experiment is that we want to observe if the amount of gas in the car affects the mileage of the car. Maybe, having less fuel in the tank might help getting us a better mileage. This is an example of how the design of experiments might help us answering some questions in our day-to-day life.

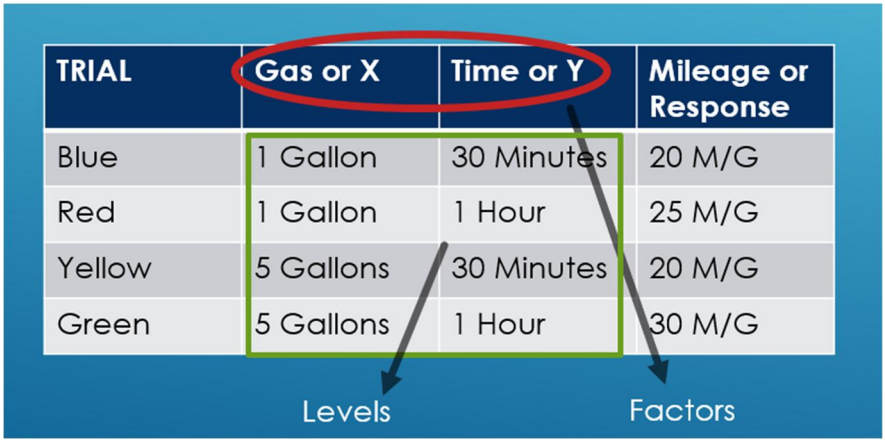

Figure 5: Design Table

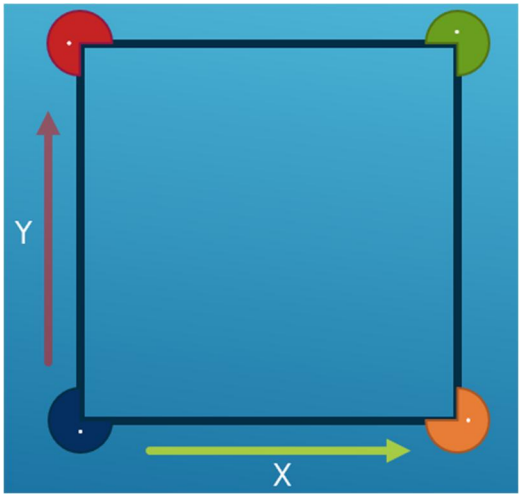

Figure 6: Experimental Design

2.6. Understanding and Calculating Factorial Effects

The effect of a factor is the change in the level of the factor causing a change in the response variable. The effect caused by a factor itself is called a main effect. While the effect caused by an interaction is called an interaction effect.

Through the viewpoint of my thesis, I have used Least Squares Estimation to understand the factorial effects for a linear regression model. For example, using the car mileage experiment from before, the linear regression model would look like this:

$$\boldsymbol{y = \beta_0 + \beta_1 x_1 + \beta_2 x_2 + \beta_{12} x_1 x_2 + \in}$$

where, β_i is the weighting factor for a variable to the response variable. The last term (β_{12}) signifies the interaction effect caused by the variables 1 and 2.

2.7. Fractional Factorial Effects

This is a common method used when the number of variables to study is large. For example, for an experiment with a 2-level design and 20 variables, the effects would number up to more than a million. A dilemma most experimental investigators face is the need to examine all combination of design factors when there are not enough resources to do so (Gunst and Mason 2009). Therefore, fractional factorial designs are of immense value. These designs make use of known properties to selectively reduce the size of an experiment while limiting the trade-off of critical information (Gunst and Mason 2009). This helps us make an economic use of our resources, identify the critical factors of our experiment, and manage the knowledge gains from our learnings.

2.7.1. Aliasing of Effects

This is one of the major drawbacks of the fractional design. When multiple columns of a design matrix correspond to each other, the effects are known to be 'aliased' with each other (Fisher 1937). This leads to problem where the magnitude of one effect cannot be differentiated from the other effect. These are called

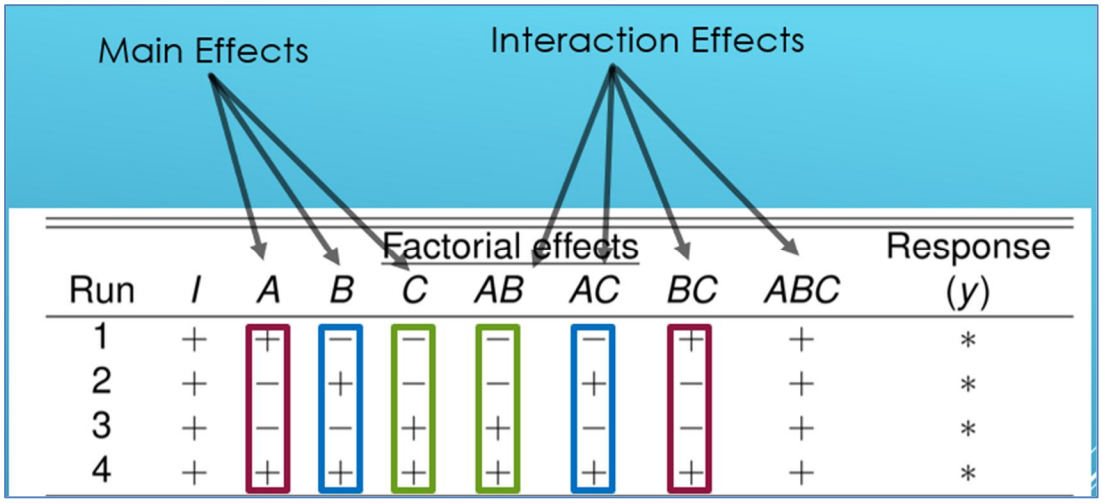

Figure 7: Fractional Factorial Design Table

confounded effects, and in such a situation no unique solution is present to estimate all the effects.

Therefore, we can assume to neglect these other effects to understand the effects we require to study.

As we see in Figure 7, for a 3-factor design, we are accounting for three main effects and four interaction effects. However, since we do not have a full factorial design, there is aliasing of the effects. As we see from the columns, that A = BC, B = AC and C = AB. Therefore, the effects of the main effect A are confounded with the interaction effect BC.

2.7.2. Effects to Neglect?

So, how do we decide which effects to neglect? And what is the rationale behind them? This is understood by three additional principles:

- Hierarchical Ordering, the lower order effects are more likely to be important than higher order ones, and effects on the same order are likely equally important.
- Effect Sparsity, number of relatively important effects is small.
- Effect Heredity, if a parent factor is significant, then it is possible for an interaction effect to be significant.

2.8. Design Generation

Generally, while generating a fractional factorial design, it is advisable that the main effects and the 2-factor interactions be estimated, while any higher order interactions neglected. An equation based on which the design is generated is called the Generator or the Defining Relationship of the design (Shah, Kulkarni et al. 2000). This equation is derived from the highest order interaction term and used to segregate the design. For example, for a 3-factor design, the equation can be I = ABC. In this equation, ABC is the Defining Word of the design.

2.9. Design Resolution

To understand the resolution of a design, we make use of the Defining Word Length. The Defining Word Length is the number of letters in the Defining Word introduced in the previous subpoint (Shah, Kulkarni et al. 2000).

From this defining word length, The Design Resolution is the smallest word length of the defining words associated with this design. The resolution benchmarks the capability in estimating the factorial effects.

For example, a resolution 3 design, has the smallest word length (I = ABC) as 3. While for a resolution 5 design, the word length (I = ABCDE) is 5. A higher resolution design leads to a clearer and better design. Shown in figure 8, is a design resolution evaluation table. It defines the resolution for a 2-level design for several factors and the required simulations respectively.

It is recommended to generally use a design with a resolution of more than 5, since the main effects and the 2-factor interactions are cleared from each other and are only aliased with 3-factor or higher order interactions.

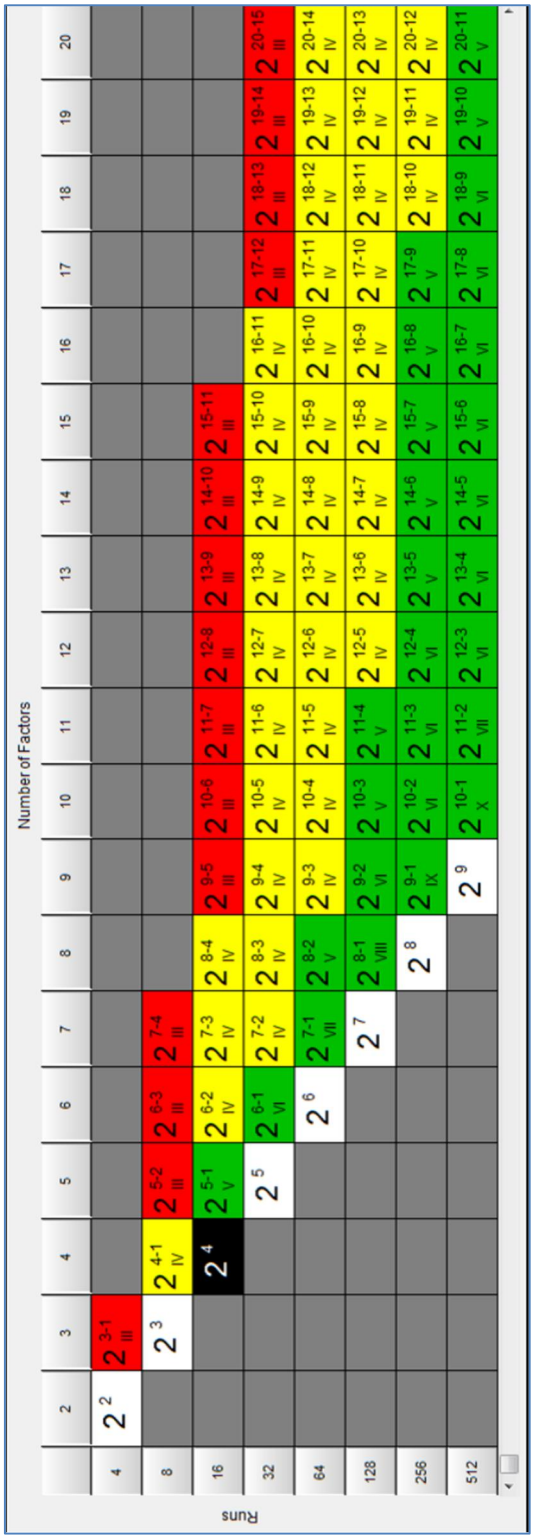

Figure 8: Design Resolution Table

Figure 8 has been obtained using a software called Minitab which is a command and menu driven statistical analysis package. Minitab helps analyzing results and examine data to make predictions from a variety of methods (Minitab 2013).

2.9.1. Clear Effects

A main effect or 2-factor interaction is cleared if none of its aliases are confounded with a main effect or a 2-factor interaction.

2.9.2. Strongly Clear Effects

A main effect or 2-factor interaction is strongly cleared if none of its aliases are confounded with a main effect, 2-factor interaction, or a 3-factor interaction.

2.10. Central Composite Design (CCD)

CCD is the most common technique to estimate a full second order model. It uses the 2-level factorial design and combines it with center points and twice the amount of factor star points. A second order model here is defined as a linear model with interactions summed with the quadratic terms. The star points help in the estimation of the curvature and signify the extreme values for a factor (Asghar, Abdul Raman et al. 2014). The distance of these star points from the center points is given by α (alpha), which is generally greater than 1. The value of alpha is generally calculated to be the root value of the number of factors (k).

The center points on the other hand are dependent on the required properties from the experiment. As though for a simulation, where they will provide the same values, 1 center point will suffice. The figure 9 below describes how the CCD experiment is setup, one can see the star points referred before at distance of root 2 from the center.

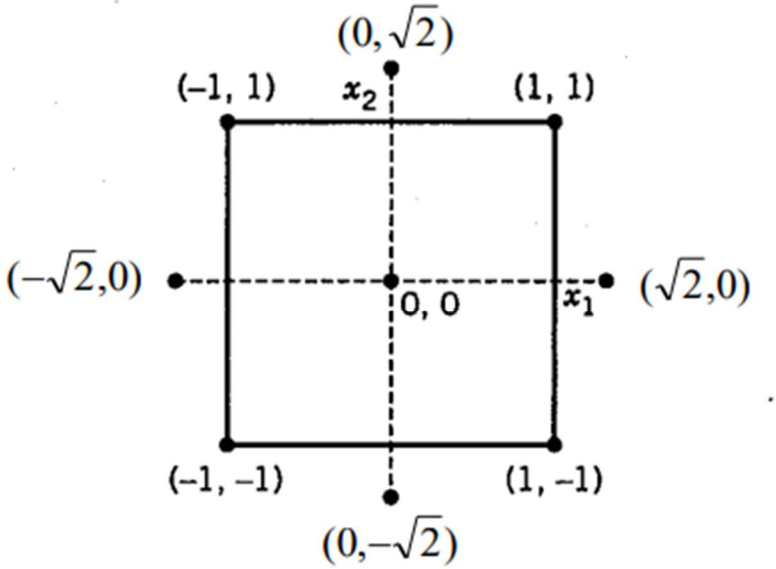

Figure 7.4 Central composite design for $k = 2$ and $\alpha = \sqrt{2}$.

Figure 9: Central Composite Design example with the star points

3. METHODOLOGY

3.1. Least Squares Estimation

For linear regression models of the form:

$$\boldsymbol{y} = \boldsymbol{\beta_0} + \boldsymbol{\beta_1 x_1} + \boldsymbol{\beta_2 x_2} + \cdots + \boldsymbol{\beta_n x_n}$$

We are generally provided the y and x values. Our aim is to find out further about the weight component β. To understand β, we use the method of least square estimation, where the squared error of the prediction is minimized. For all N observations, we get:

$$\boldsymbol{Y} = \boldsymbol{X\beta}$$

The difference between the observed values with the predicted values is the prediction error and the least squares tries to minimize the sum of these errors.

For $\boldsymbol{X}$ being the matrix containing the values of $\boldsymbol{x}$ and $\boldsymbol{Y}$ being the matrix containing all the values of $\boldsymbol{y}$, the $\boldsymbol{\beta}$ can be obtained by:

$$\boldsymbol{\beta} = (\boldsymbol{X^T X})^{-1} \boldsymbol{X^T Y}$$

3.2. Least Squares Estimation for Effect Estimation

For cases of design of experiments, to utilize the LSE for effect estimation, we make use of switching variables. These variables only take the value of 1 or 0, indicating whether the variable is active or not. Therefore, the total number of switching variables available should be the sum of the level values of the factors included in an experiment.

3.3. Factorial Effects and Plots

A factorial effect is defined as the change in the response produced by a change in the level on that the factor or interaction, averaged over the levels of the other factors.

Main effect is the effect of a factor itself; it is given by:

$$\boldsymbol{ME(A) = \overline{Z}(A = +) - \overline{Z}(A = -)}$$

In the equation above, Z is the value of the response variable, and $\boldsymbol{\overline{Z}(A = +)}$ is the average of the response variable when main effect A is switched on, and vice versa.

Similarly, the interaction effect is given by:

$$\boldsymbol{INT(AB) = \overline{Z}(AB = +) - \overline{Z}(AB = -)}$$

3.4. LSE Estimate for Factorial Effects

To compute the factorial effects using LSE, we assume a regression model to use. For a 2-factor experiment, where we would like to estimate the main and interaction effects, we would use the following model:

$$\boldsymbol{y = \beta_0 + \beta_1 x_1 + \beta_2 x_2 + \beta_{12} x_1 x_2}$$

Where, the second and third term on the right are the main effects, while the last term is the interaction effect. We use a vector-matrix format to solve the equations:

From the design matrix

Run	I	x_1	x_2	x_1x_2
1	1	-1	-1	1
2	1	1	-1	-1
3	1	-1	1	-1
4	1	1	1	1

Figure 10: Example Design Matrix

Here we have the design matrix, and will write this in a matrix form:

$$\mathbf{X}_{unreplicated} = \begin{bmatrix} 1 & -1 & -1 & 1 \\ 1 & 1 & -1 & -1 \\ 1 & -1 & 1 & -1 \\ 1 & 1 & 1 & 1 \end{bmatrix}$$

Figure 11: Design Matrix in Matrix Form

3.5. Response Surface Methodology

For the 2-level designs, only the linear effect can be studied from the response surface. In the figure below, one can see that by only having 2 levels for a variable, only a linear response can be obtained.

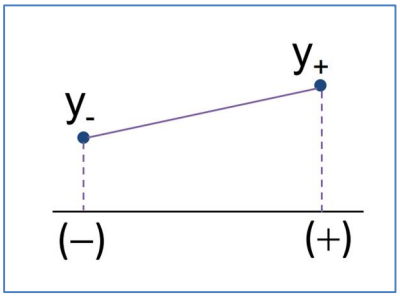

Figure 12: Level Estimation

Therefore, to check for curvature we need to have a few quadratic terms in the model and maybe have more than 2 levels.

Response surface methodology is a sequential strategy to use a simple model to represent the response surface and investigate the entire surface. RSM is used for complicated problems as it is difficult to use a second order model alone to represent a

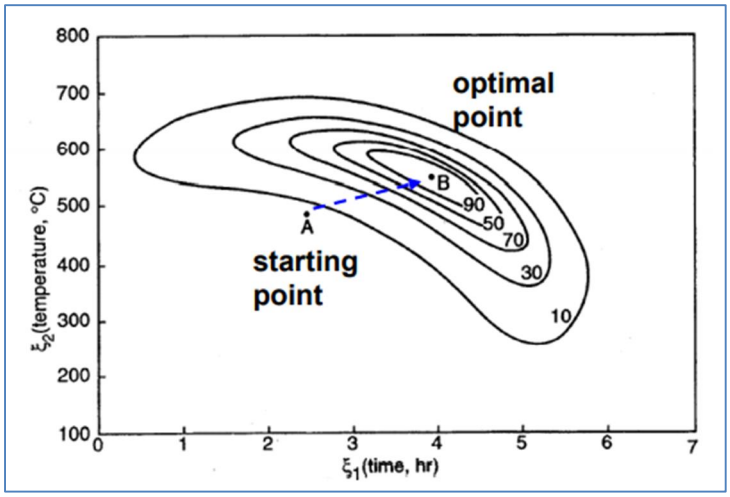

Figure 13: Response Surface

response in the entire design.

RSM consists of a group of mathematical and statistical techniques used in the development of an adequate functional relationship between the response of interest and a number of associated control variables (Khuri and Mukhopadhyay 2010). In figure 13 above, this technique has been shown very elegantly and presents how multiple iterations work to find the optimal point.

3.6. Compositional Reservoir Flow Simulation

The simulator used for this study is a multi-component multi-phase fluid transport reservoir simulator. The simulator considers the organic matrix in the continuum and hydraulic fractures as discontinuous. It is assumed that the organic matrix is surrounded by the inorganic matrix and for the hydrocarbons to be transported through the matrix, they need to move through the inorganic matrix. The simulator predicts the pressure and composition dependence based on the Maxwell-Stefan diffusion theory. The partial

differential equations are discretized using the control volume finite element method in space and the temporal discretization is make done using a fully implicit backward Euler scheme.

A multi-component heavy gas mixture has been used for our experimentation consisting of methane, ethane, propane, butane, and pentane representing a higher specific gravity.

Model fluid	CH_4	C_2H_4	C_3H_8	C_4H_{10}	C_5H_{12}
Component Fraction	0.54	0.166	0.128	0.107	0.059

Table 1: Reservoir Fluid Composition

3.7. Reservoir Model

This study has been conducted in two phases and the model considers a single hydraulic fracture, vertical to the well. For our case we have gone for the most common case seen in the field, one with high fracture conductivity and low matrix permeability. Fracture conductivity gives us an idea of how easily fluids can be transmitted through propped hydraulic fractures (Warpinski, Mayerhofer et al. 2009). It is directly proportional to the fracture permeability and the fracture width providing us the with the more commonly used term for dimensionless fracture conductivity:

$$C_{fD} = \frac{k_f w_f}{k_m X_f}$$

Here, k_f is the fracture permeability and w_f is the fracture width

The 1st phase considers 15 parameters that range from rock and fluid properties, hydraulic fracture properties, and wellbore conditions.

The reservoir model has been simulated in NaSh, which indicates the flow through the fracture. NaSh can indicate the flow by calculating the pressure around the fracture. It uses a variable mesh system where the grid sizes are much smaller closer to the fracture tips to account for rapidly changing pressures.

Using the pressure profile, NaSh calculates the cumulative production over a given period. As shown in figure 14, the cumulative gas production has been calculated over a period of 5 years for example.

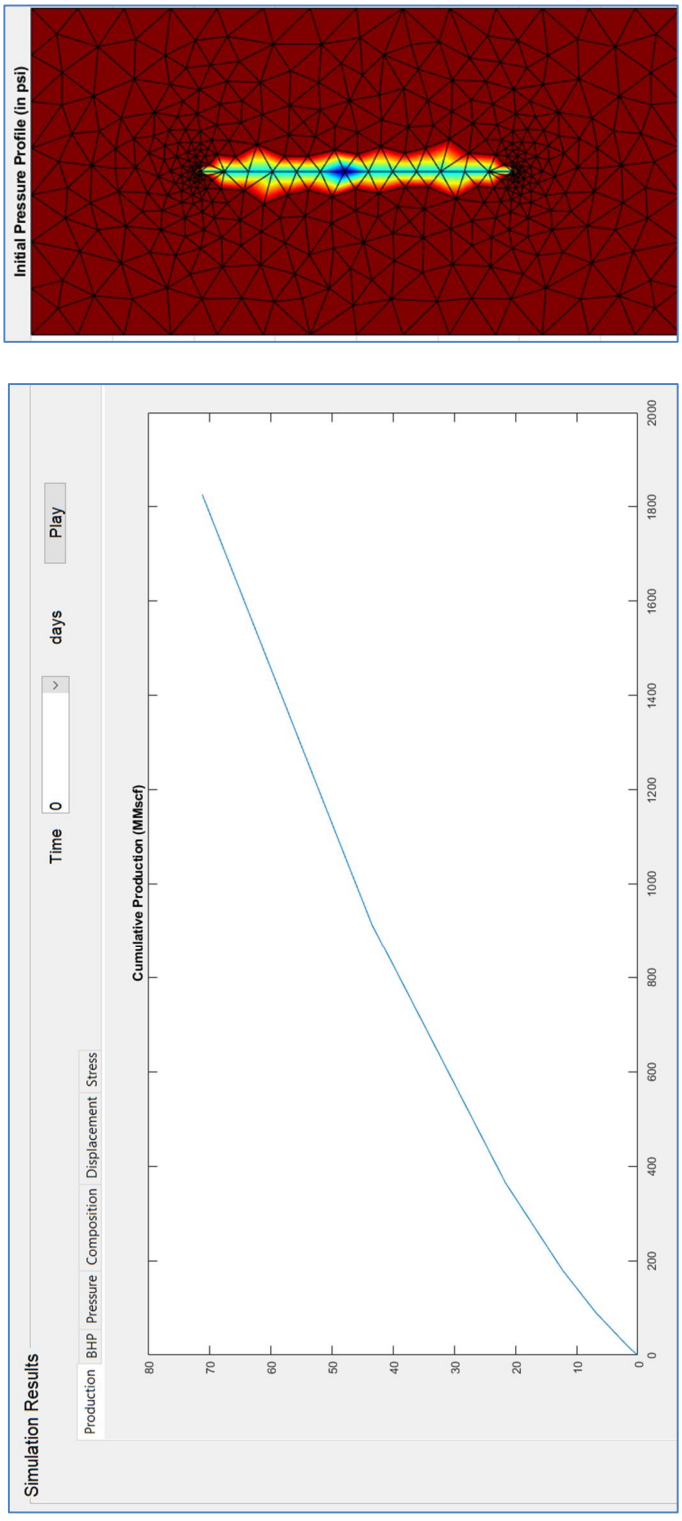

Figure 14: Example simulation from NaSh, with the resulting Cumulative Production graph

The values for the parameters are based upon those from the Barnett Shale formation. For phase 1, a resolution 4, 15 variable-2 level fractional factorial design has been selected for testing. This design required 32 runs. In table 2 below, one can find the summary of the 15 parameters used for the initial experimentation.

The parameters related to propped hydraulic fracturing are:

- Fracture Permeability
- Fracture Width
- Fracture Young's Modulus
- Fracture Half Length
- Fracture Poisson's Ratio
- Fracture Porosity

Other variables taken into consideration include the maximum confining stress, which affects the matrix permeability and the m exponent value. Both are introduced in our consideration as part of Gangi's permeability model. Geo-mechanically we have taken into consideration properties such as Young's Modulus and Poisson's Ratio as they are related to proppant distribution and contacts between the grains and the wall.

Symbol	Parameter	Base	Multiplier			Unit
		Value	Case Values	High level	Low level	
A	Fracture permeability	5.00E-11	10^0.001	6E-13	4E-13	m^2
B	Fracture width	0.003	1	0.0036	0.0024	m
C	Max confining stress	14000	1	16800	11200	psia
D	Fracture Young's modulus	4.00E+03	1	4800	3200	
E	Fracture half length	120	1	144	96	m
F	Fracture Poisson's ratio	0.25	1	0.3	0.2	
J	Viscoelastic shear coefficient	6.80E+09	1	8.16E+9	5.44E+9	Mpa/S
H	m exponent	0.4	1	0.48	0.32	
J	Poisson's ratio	0.25	1	0.3	0.2	
K	Young's Modulus	4.00E+04	1	48000	32000	Mpa
L	Matrix permeability	2.47E-15	0.001	2.964E-18	1.976E-18	m^2
M	Matrix porosity	0.054	1	0.0648	0.0432	
N	Bottomhole pressure	13.7896	1	16.54752	11.03168	Mpa
O	Fracture porosity	0.33	1	0.396	0.264	

Table 2: Parameter Experimental Values for Phase 1

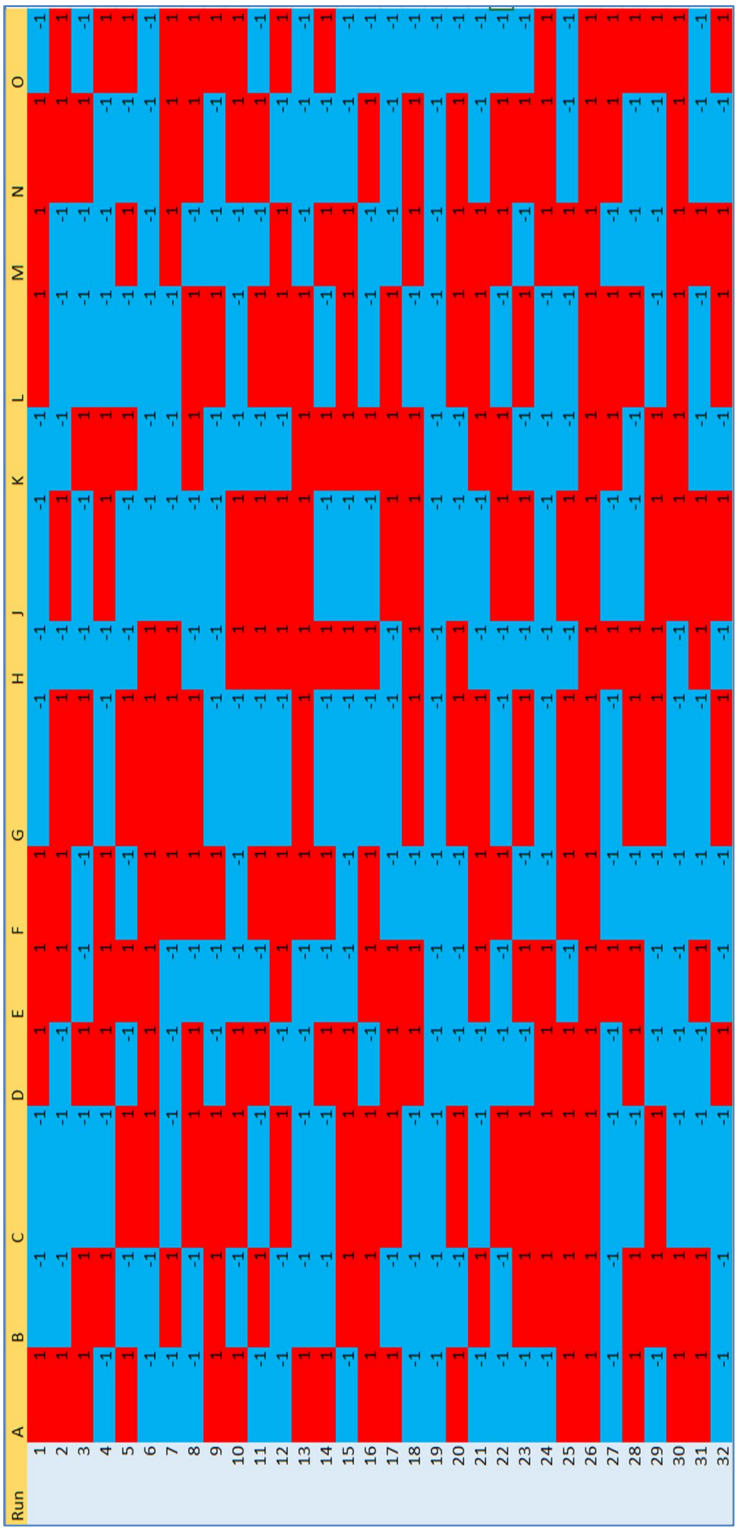

Figure 15: Experimental Design for Phase 1

The second phase considers the 10 most important parameters seen from the study in the first phase experimentation which can be found in table 3 below. The second phase is a more complicated Central Composite Design experiment to further understand the importance of these 10 variables and how they affect the response variable. The CCD Experiment helps us look for a more complex relationship with the response variable.

Symbol	Parameter	Base	Multiplier			Unit
		Value	Case Values	High level	Low level	
A	Fracture permeability	5.00E-11	10*0.001	6E-13	4E-13	m^2
B	Fracture width	0.003	1	0.0036	0.0024	m
C	Max confining stress	14000	1	16800	11200	psia
D	Fracture half length	120	1	144	96	m
E	m exponent	0.4	1	0.48	0.32	
F	Young's Modulus	4.00E+04	1	48000	32000	Mpa
G	Matrix permeability	2.47E-15	0.001	2.964E-18	1.976E-18	m^2
H	Matrix porosity	0.054	1	0.0648	0.0432	
I	Bottomhole pressure	13.7896	1	16.54752	11.03168	Mpa
K	Fracture porosity	0.33	1	0.396	0.264	

Table 3: Parameter values for Phase 2 experimentation

4. EXPERIMENTAL RESULTS

4.1. Phase 1: 15 Variable Fractional-Factorial Design

The sensitivity analysis was done by changing $\pm$ **20**% for the variable level $\pm$ **1**. Since we were using a resolution 4 design, the simulation results for all the 32 runs were observed after 1 and 3 years of production. Using a linear regression model, I calculated the beta weighting factor using least square estimation for each variable, which represents how sensitive the response variable is to that parameter. A higher beta value represents a higher sensitivity to the response variable. In the graph below, the cumulative oil production is shown with every simulation and different parameter values.

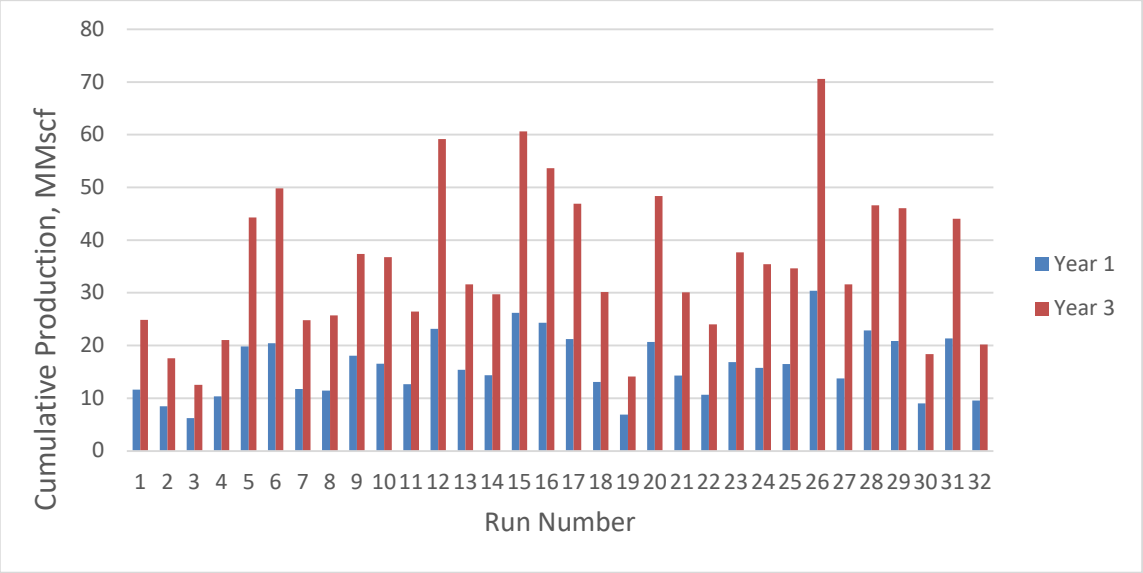

Figure 16: Cumulative Gas Production for Phase 1

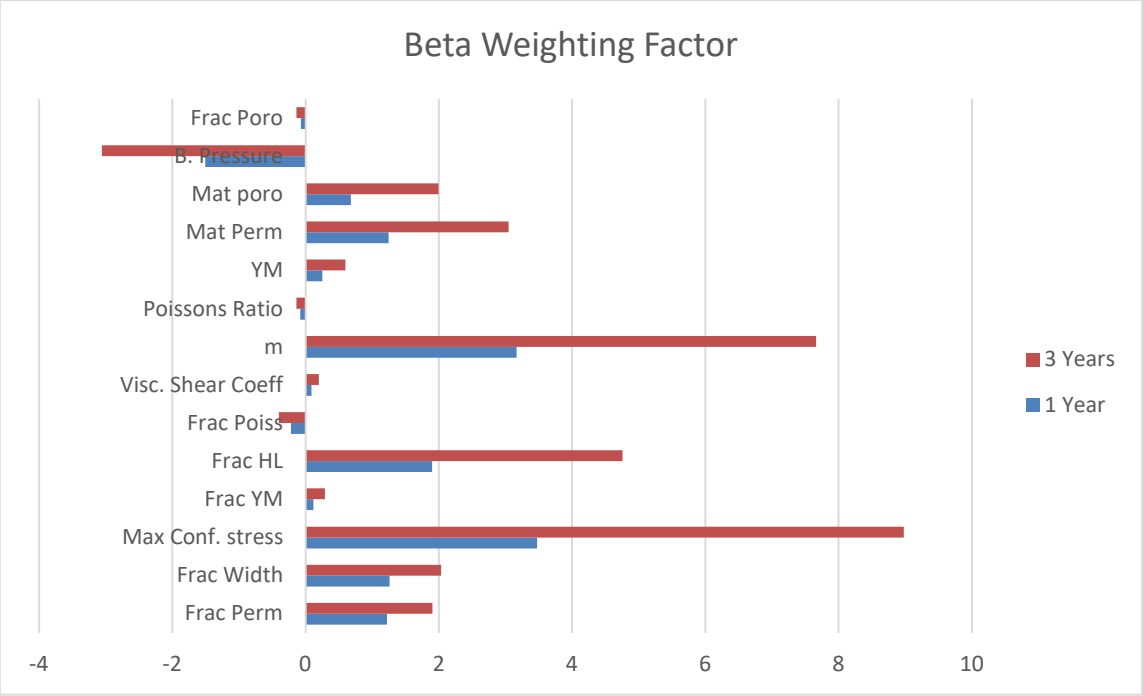

Figure 17: Weighting factors for the parameters in Phase 1

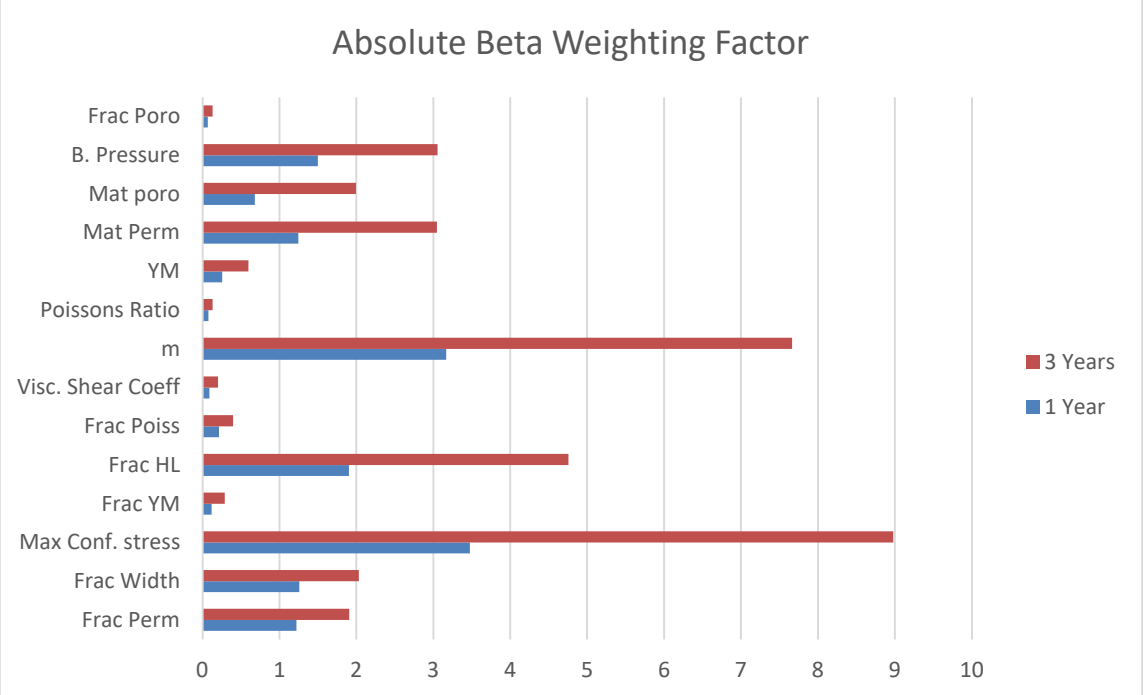

Figure 18: Absolute weighting factors for the parameters in Phase 1

Using the cumulative oil production as the response variable, I achieved my goal of finding the beta weighting factors for each of the parameters.

In the graphs above, we can see the weighting factors after 1 and 3 years respectively.

After 1 year of oil production, we observed that oil production has the highest sensitivity to the maximum confining stress from hydraulic fracturing, while the *m* exponent is a close second behind. Both of which are related to the stress-dependent permeability indicating that the biggest contributor for shale gas transport is the stress-sensitive matrix permeability. Increasing the values of these parameters would imply the need for higher resistance to shut-off the pores. Fracture half-length comes in at 3rd place as a higher half-length would mean an increase in surface area of the fracture leading to increased flow of fluids. Bottom hole pressure is 4th as it controls the flow of gas from the well and matrix permeability comes after and closes out the top five most sensitive variables. The matrix permeability controls how easily the gas flows through the matrix from the organic matter into the fractures.

Looking to 3 years after oil production, we observe an increasing dominance of the maximum confining stress and the m exponent. This is relative to the fact that as gas production increases the cracks dominated pore space starts to close out and the dependence on the stress-sensitive permeability increases and becomes more sensitive. We can see that over time the dominance of fracture half-length has increased, this is in reason for the fact the higher the fracture half length, the longer it will take for the fracture to shut-off.

Looking at the results obtained from above, we can see that the five least sensitive parameters are:

- Fracture Young's Modulus
- Fracture Poisson's Ratio
- Matrix Poisson's Ratio
- Fracture Viscoelastic Shear Coefficient
- Large Pore/ Nanopore Threshold in the matrix

Poisson's ratio was removed as it measures the deformation in the direction perpendicular to the direction of the applied force, which is dependent on the quality of the material and is something we cannot control and measure at each fracture, as it would change. Similarly, the hydraulic fracture's Poisson's ratio should also be removed.

The Fracture's Young modulus was also removed from the list as it is dependent on the quality of the material. It indicates elasticity of the propped hydraulic fracture, which should not be of concern as once we have fractured it, it will not remain elastic.

The fracture viscoelastic shear coefficient has been removed because its once the fracture has formed the material has been deformed and will not affect gas production.

These variables were not as sensitive to the response variables, therefore have been discarded from changes in Phase 2 of the experimentation (They are still taken into consideration for the rest of the experiment but are not changed with each simulation). The values of these variables have been fixed to the base values as mentioned before.

4.2. Phase 2: 10 Variable-Central Composite Design

The sensitivity analysis was done by changing $\pm \mathbf{20}\%$ for the variable level $\pm \mathbf{1}$ and the simulation results for all the 160 runs compared were observed after 1 and 3 years of production. For the central composite design, to look for any curvature in relation to the response variable, the sensitivity analysis considers changing the variable to $\pm \sqrt{\mathbf{2}}$ level to the deemed star points. These star point values help us gain better insight into the most important variables which affect gas production from fractures and how they change over time. The simulations were run in NaSh, and the results have been processed in a software called Minitab provided by the TAMU College of Engineering.

In the graph below, the cumulative oil production is presented for each of the 160 simulations. The simulations were running in a randomized order.

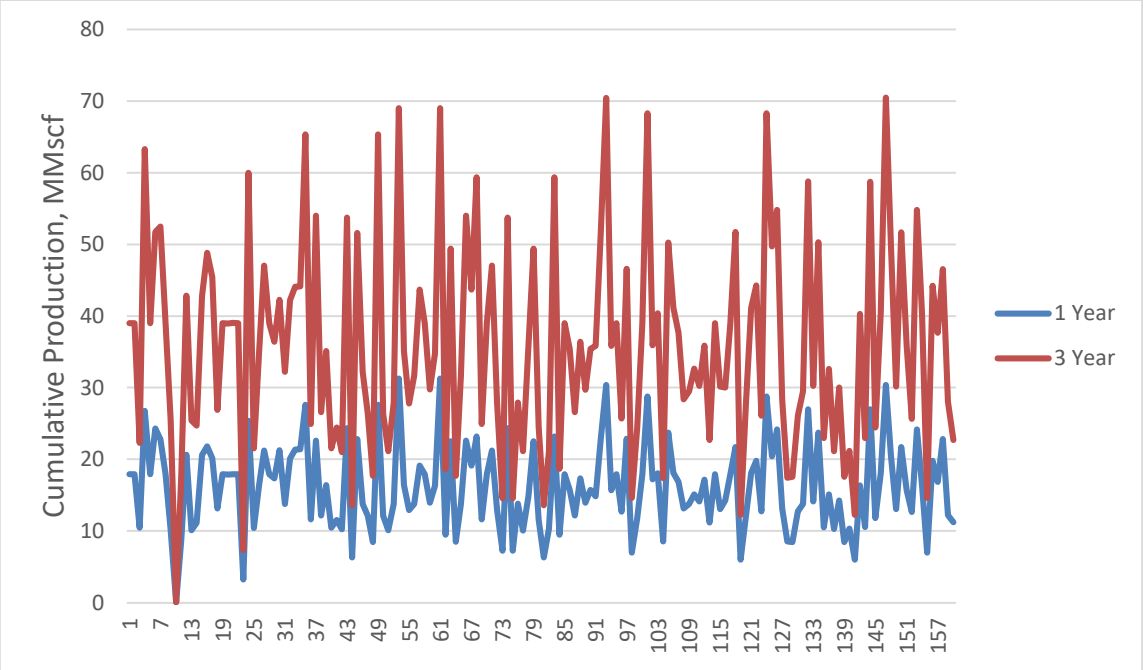

Figure 19: Cumulative Production for Phase 2 of the Study

Using the cumulative production data, we have put the data into Minitab and applied a design of experiment analysis. This gives us our most important variables for gas production after one year, which can be seen on the pareto chart in Figure 20. Maximum confining stress and m exponent still take the top spots followed by fracture half length, bottom hole pressure and matrix permeability after gas production for one year.

One of the most surprising finds is that the hydraulic fracture porosity and young's modulus are not nearly as important as most of the other 2-factor interactions. Also, if we look closely, fracture permeability is one of the weaker variables, however, the 2-factor interaction of fracture permeability and maximum confining stress is much higher than the other two-factor interactions.

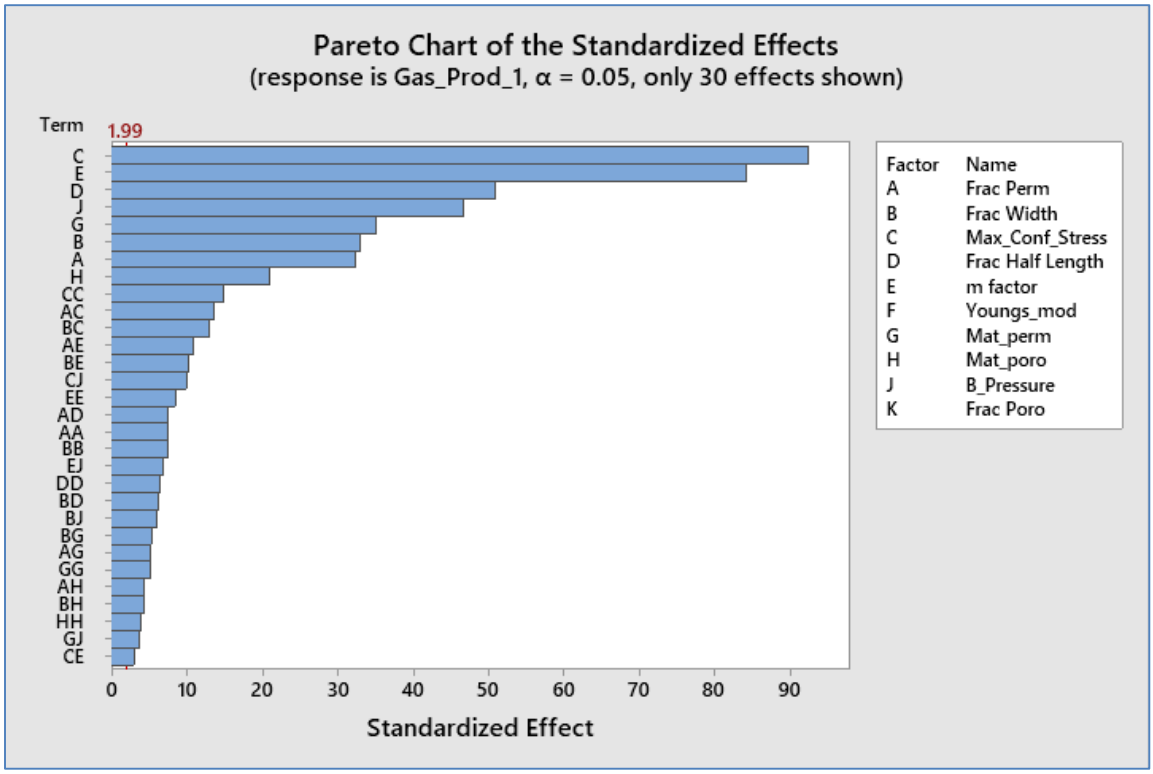

Figure 20: Pareto chart showcasing the weights of different effects after 1 year of production

Similarly, looking at the results for gas production after three years, we get the pareto chart in Figure 21 below. The maximum confining stress and m exponent have increasingly become sensitive to the response variable over time and dominant. Fracture half-length, bottom hole pressure and matrix permeability close out the top five again.

However, on observation we can see that the matrix porosity has become stronger than fracture permeability and fracture width. This is possible that over time as fractures start to shut-off, the matrix porosity becomes more important for shale gas transport. Most of the results we have seen are pretty much in line with what we saw in the fractional factorial design experiment.

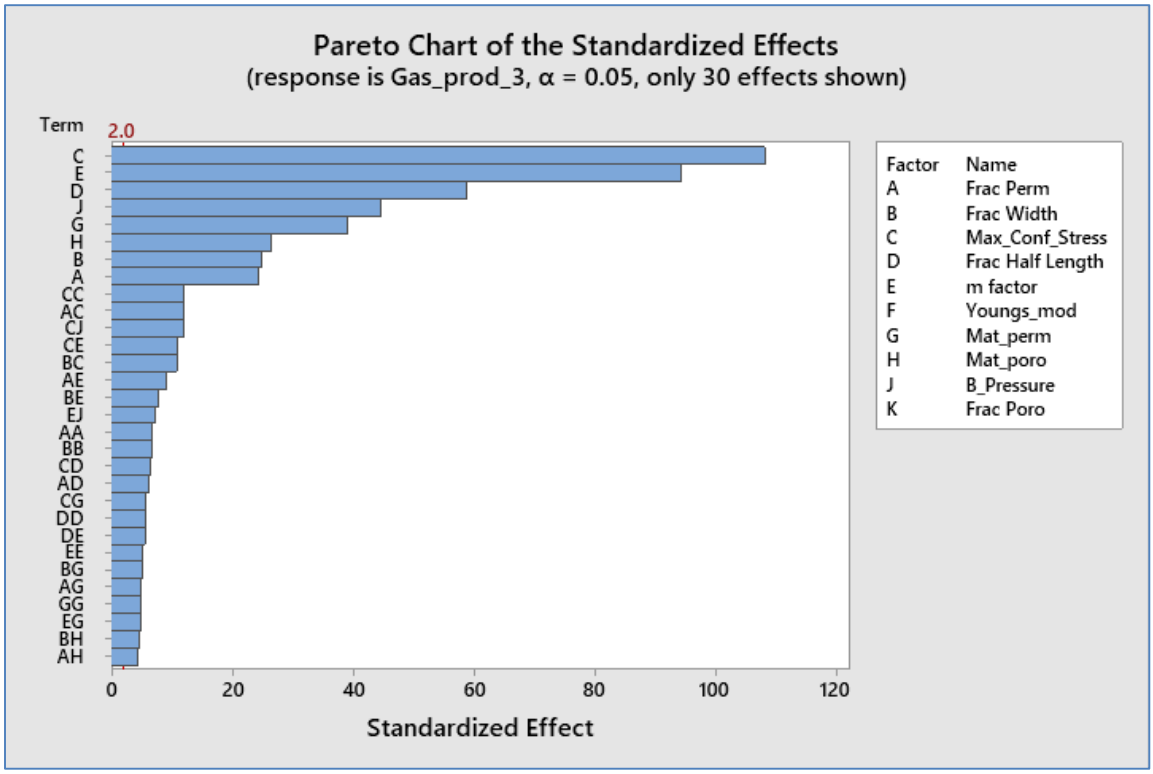

Figure 21: Pareto chart showcasing the weights of different effects after 3 years of production

Now, we will be looking into why we are using the central composite design process. CCD helps us understand the relationship of the variables with the response variable. In fractional factorial we could only see a linear relationship, however on completing our central composite design experiment, the relationships have turned out not to be linear and in fact there is a curvature. In figure 21 and 22, we can see the main effects plot for cumulative gas production after 1 and 3 years, respectively. Except for Young's modulus and fracture porosity, the variables have a non-linear relationship with the gas production, changing over time as well. The non-linear model indicates that the linear model is actually an approximation for a higher order model. In figure 22, we can see that

for the factors other than Youngs' Modulus, Fracture Porosity and Bottomhole Pressure, we see a positive relationship with the gas production over time. The graphs are initially showing a linear behavior and then start to flatten out. For the case of Bottomhole pressure, we see a negative relationship with the gas production, while for Youngs' Modulus and Fracture Porosity, we see the graph totally flat implying there is no relationship.

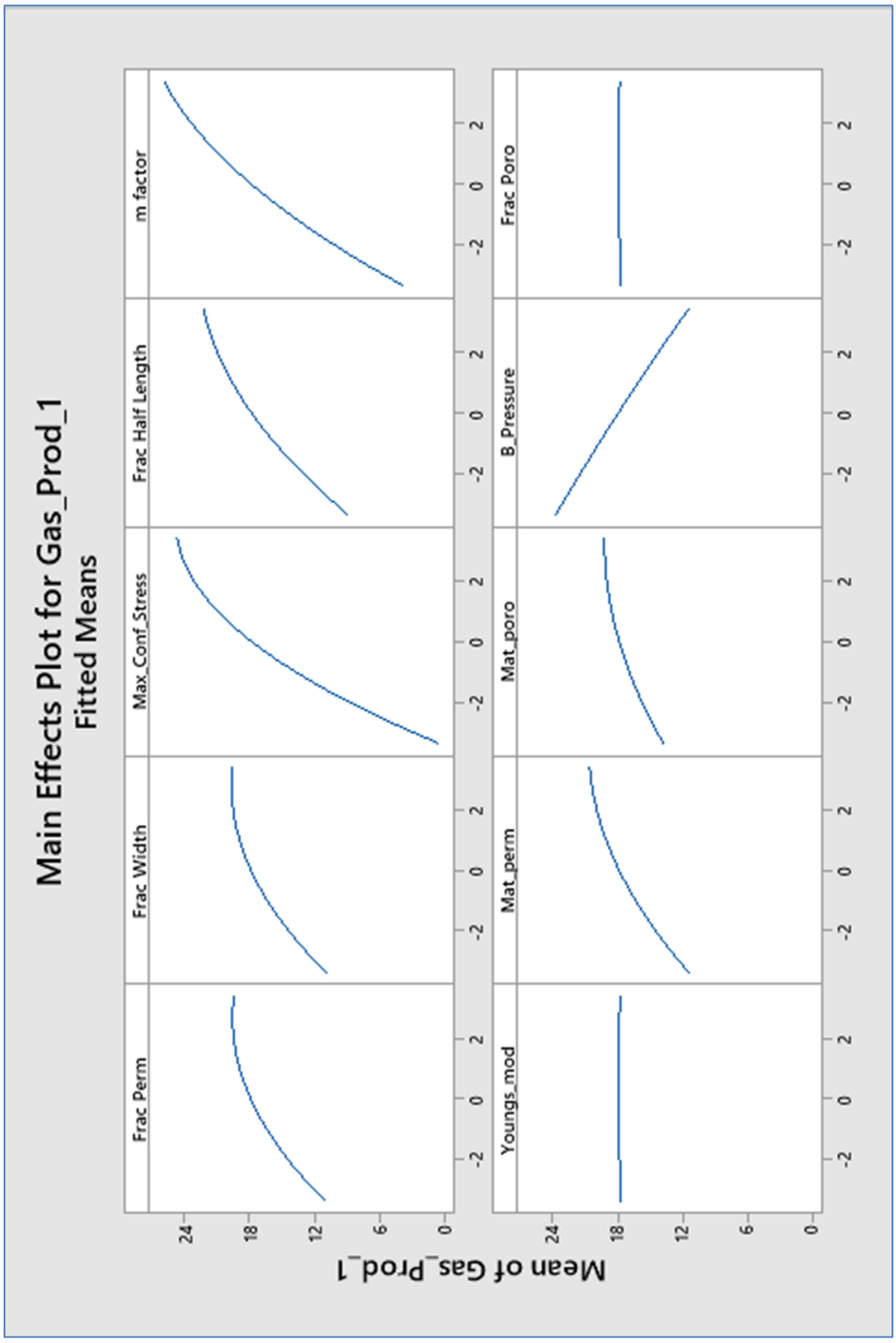

Figure 22: The relationship of the main effects with the cumulative gas production after 1 year of production from the well

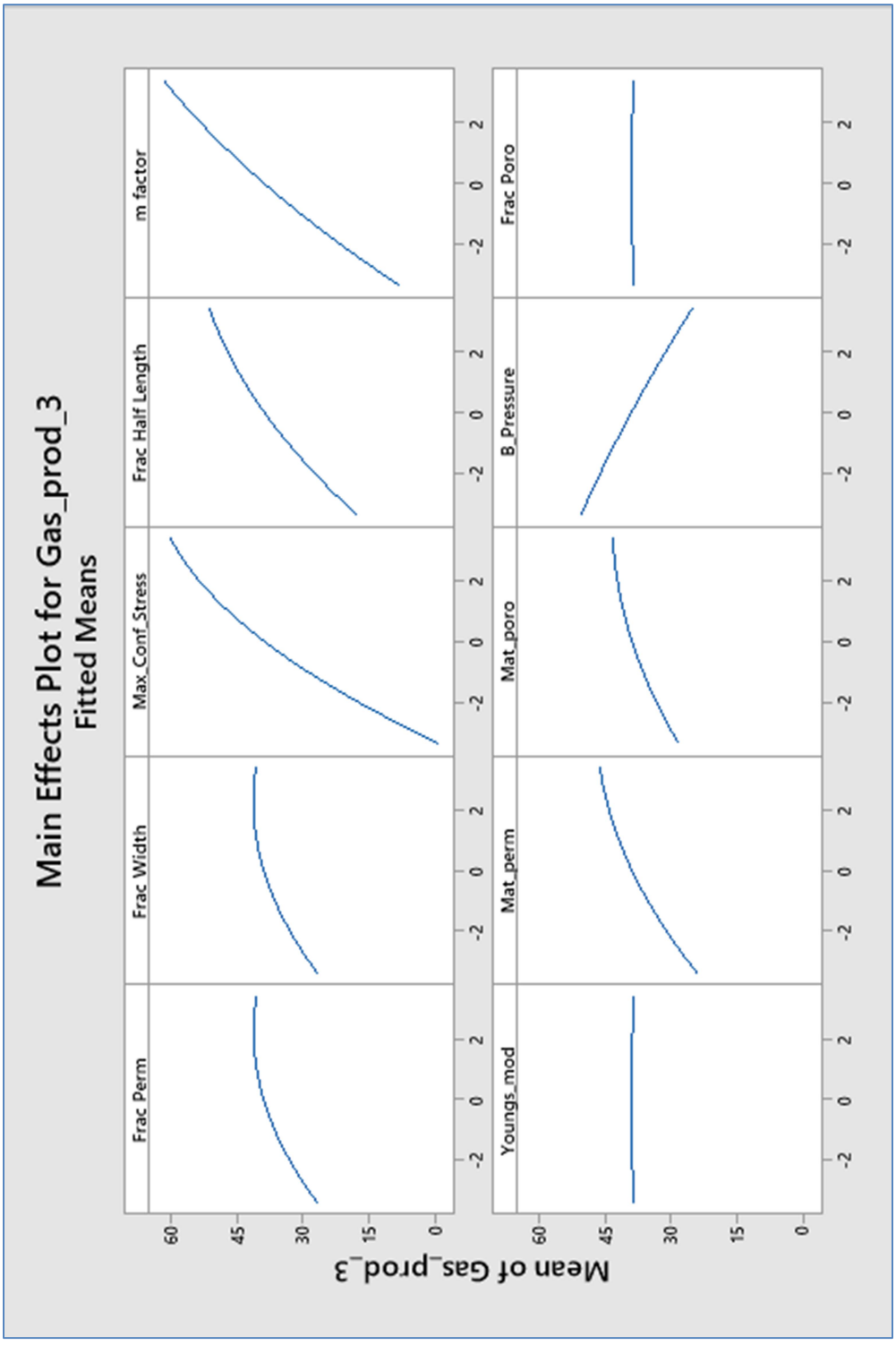

Figure 23: Describes the relationship of the main effects with cumulative gas production after 3 years

One interesting observation from the above results is that there is an apex for the curve of the hydraulic fracture permeability and the fracture width. Implying that increased fracture permeability and fracture width will not change oil production after a threshold point (near +2) and therefore, there is an optimum value for these two parameters.

A possible explanation for the apex seen in the fracture width and the fracture permeability relations could be that as the hydraulic fracture's conductivity is increased significantly at one point the fracture reaches an infinite-conductivity flow condition, when the fracture becomes insensitive to the permeability and width.

The behavior of the other variables is what we expected intuitively. The maximum confining stress and the *m* factor have a strongly dominating effect on the oil production, increasing with higher values, as well as fracture half length, matrix porosity and matrix permeability.

Minitab was also able to run an ANOVA (Analysis of Variance) on the dataset and provided us with the following values. Looking at the ANOVA table, we can distinctly see the P-Values for the Youngs' Modulus and Fracture Porosity to be very high. The P-Values are generally very high for variables which do not affect the response variable in the model and values can range from 0 to 1. Such a high P-Value indicates that both the variables should not be used for characterizing the model.

Analysis of Variance

Source	DF	Adj SS	Adj MS	F-Value	P-Value
Model	65	32528.4	500.4	473.11	0.000
Linear	10	31130.9	3113.1	2943.12	0.000
Frac Perm	1	629.8	629.8	595.39	0.000
Frac Width	1	645.6	645.6	610.36	0.000
Max_Conf_Stress	1	12340.1	12340.1	11666.30	0.000
Frac HL	1	3660.8	3660.8	3460.87	0.000
m factor	1	9390.2	9390.2	8877.51	0.000
Youngs_mod	1	0.0	0.0	0.00	0.975
Mat_perm	1	1619.1	1619.1	1530.67	0.000
Mat_poro	1	740.6	740.6	700.19	0.000
B_Pressure	1	2104.8	2104.8	1989.85	0.000
Frac Poro	1	0.0	0.0	0.01	0.931

Table 4: Dataset ANOVA table

Figure 24 and 25 below show how the interaction effects affect the mean gas production after 3 years. To explain more clearly, taking the example of the fracture half-length interaction with the matrix permeability (shown in the red rectangle in figure 24), the x-axis has the values for the matrix permeability, while the y axis has the values for the mean cumulative gas production. This sub-plot has 3 distinct lines, which are at the defined levels for matrix permeability (shown in the green rectangle in figure 24). Looking at the green and red line which are at the high level and center point for matrix permeability respectively when compared to the blue line which is at the lower level seem to be much closer to each other, while the blue line is further away. This indicates that the factors when increased are beneficial to increasing the mean gas production, but if reduced are more detrimental to the mean gas production.

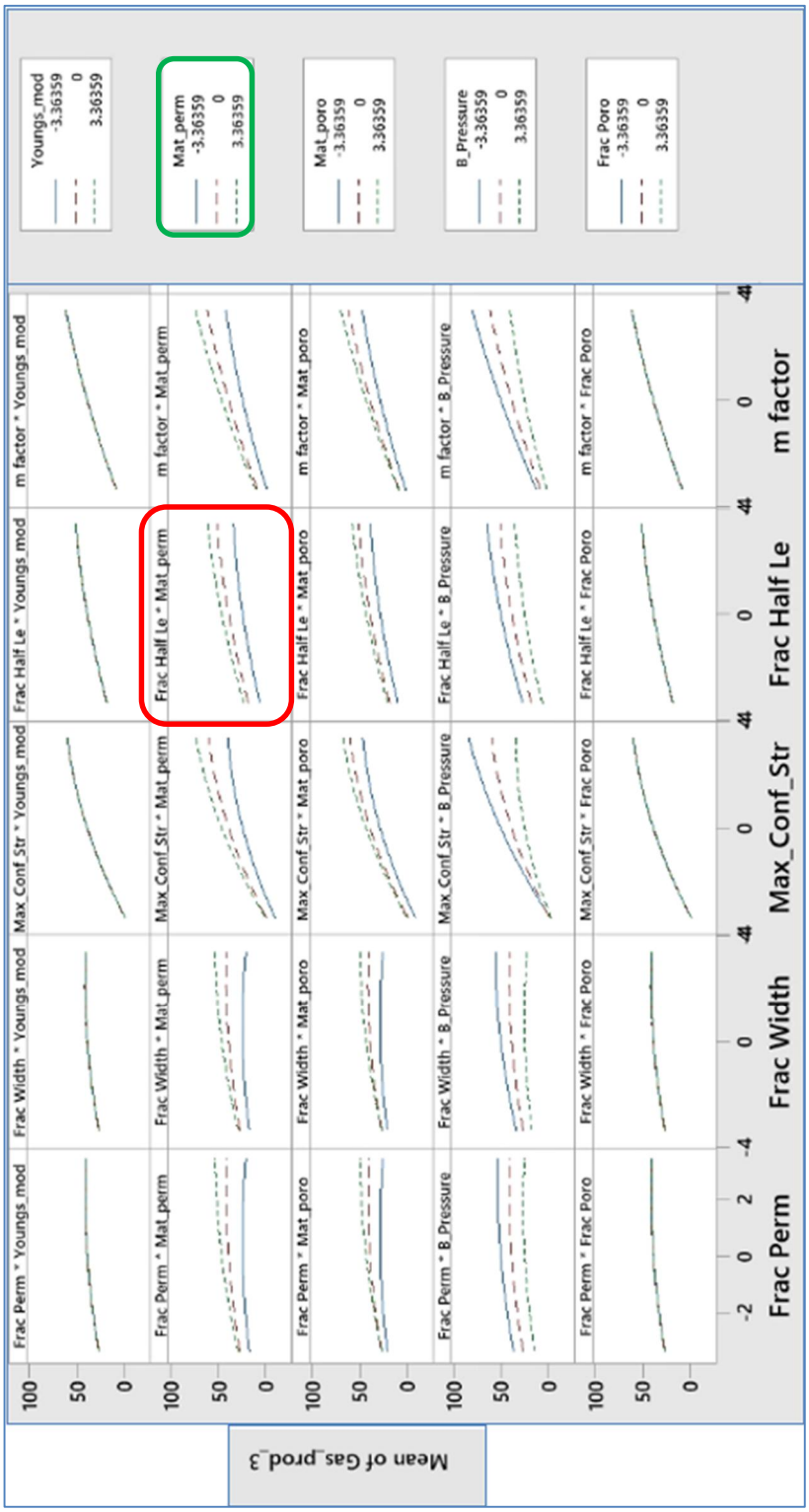

Figure 24: Interaction Effects Plot 1

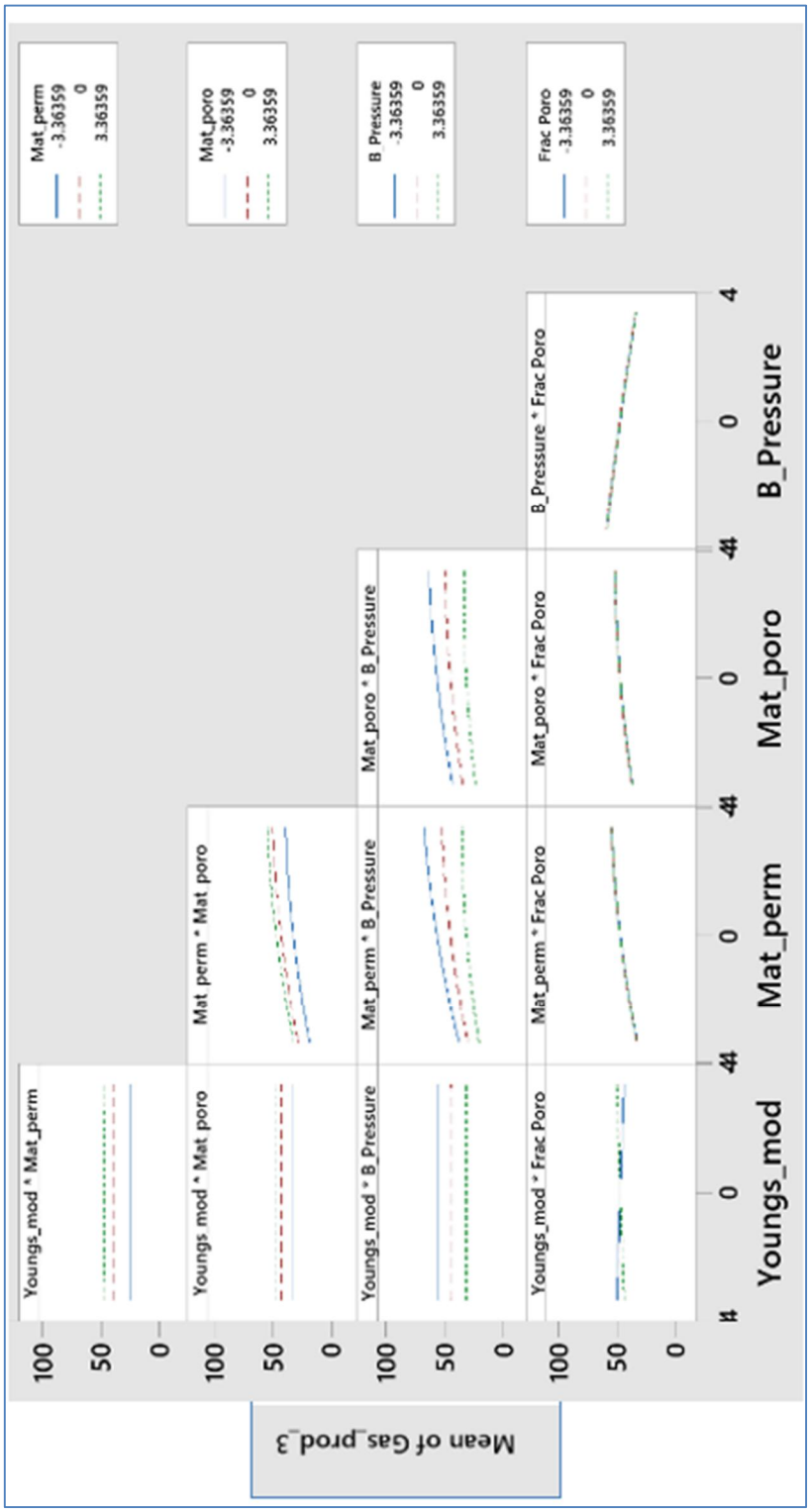

Figure 25: Interaction Effects Plot 2

Looking at the results, we can see that the cumulative gas production in shale reservoirs is a slave to the stress-dependent matrix permeability. Thus, it is important to find reservoirs with favorable reservoir conditions. We can see this from the dominance of the maximum confining stress and the m exponent on the model. Fracture half-length is the most important well completion factor under our control, and it is important to have the length as much as possible. The fractures need to be ensured they are open for as long as possible, as over time as they close out, the production becomes more dependent on the stress-dependent matrix permeability.

5. CONCLUSIONS

This sensitivity analysis experimentation was done to help us understand how various completions and petrophysical factors affect the gas production from unconventional reservoirs. The cumulative gas production has been measured after 1 and 3 years to understand the effects of the various parameters. The experimentation was done in 2 phases, the 1st phase considers 15 parameters that range from rock and fluid properties, hydraulic fracture properties, and wellbore conditions. While the 2nd phase considers the 10 most important parameters seen from the study in the 1st phase experimentation.

Based on the results, we conclude that:

- During the first phase experimentation, out of the 15 factors we used, the top five parameters were the maximum confining stress, the m exponent, the fracture half length, the bottomhole pressure and the matrix permeability.
- The maximum confining stress and m exponent are related to the stress-dependent matrix permeability, meaning that increasing them would lead to a higher resistance from the pores closing.
- The fracture half-length leads to an increase in the surface area of the fracture for increased flow of gas.
- The bottomhole pressure controls the flow of gas, while the matrix permeability controls how easily gas can flow into the fractures

- Out of these 15 factors, the bottom five were entirely non-effective being the fracture's Youngs modulus, Poisson's ratio, the matrix Poisson's ratio, the fracture visco-elastic shear coefficient and the matrix large pore/nanopore threshold.
- For the second phase experimentation, the ten most important factors were selected from the first phase, being the fracture permeability, the fracture width, the maximum confining stress, the fracture half length, m factor, the matrix young's modulus, the matrix permeability, the matrix porosity, the bottomhole pressure and the fracture porosity.
- For the second phase, we got similar results to that of the phase 1, with the top five parameters being the maximum confining stress, the m exponent, fracture half length, bottomhole pressure and the matrix permeability.
- The second phase helped us understand the relationship of the variables in much more depth with the response variable as we were able to figure a non-linear relationship. The non-linear model helps us realize that the relationship of the variables with the response is kind of linear initially and slowly turns and flattens out, while also allowing us to understand if the variable is positively or negatively related to the response.
- The maximum confining stress and m exponents become more dominating as the well produces for longer. As the well produces for longer, the fractures start to close out and the gas production becomes more dependent on stress-dependent matrix permeability.

- The fracture permeability and the fracture width achieve an optimum point where the fracture maintains an infinite conductivity and hence the production can be maximized.

REFERENCES

Aggour, T. M. and M. J. Economides (1999). "Impact of Fluid Selection on High-Permeability Fracturing." SPE Production & Facilities **14**(01): 72-76.

Akkutlu, I. Y., et al. (2017). Shale resource assessment in presence of nanopore confinement. SPE/AAPG/SEG Unconventional Resources Technology Conference, OnePetro.

Akkutlu, I. Y. and E. Fathi (2012). "Multiscale gas transport in shales with local kerogen heterogeneities." SPE journal **17**(04): 1002-1011.

Ambrose, R. J., et al. (2012). "Shale gas-in-place calculations part I: new pore-scale considerations." SPE journal **17**(01): 219-229.

Asghar, A., et al. (2014). "A comparison of central composite design and Taguchi method for optimizing Fenton process." The Scientific World Journal **2014**.

Baioco, J. S., et al. (2020). Design of Experiment (DOE) Approach to Sensitivity Analysis of Hydraulic Fracturing. 13th International Ocean and Polar Engineering Conference, OnePetro.

Bui, K. and I. Y. Akkutlu (2017). "Hydrocarbons recovery from model-kerogen nanopores." SPE journal **22**(03): 854-862.

Chidi, A., et al. (2014). Application of Design of Experiment Workflow to the Economic Evaluation of an Unconventional Resource Play, SPE.

Essien, A. and J. Akpabio (2020). Evaluating the Effects of Petrophysical Properties on Oil Initially in Place, SPE.

Fisher, R. A. (1936). "Design of experiments." Br Med J **1**(3923): 554-554.

Fisher, R. A. (1937). "The design of experiments." The design of experiments.(2nd Ed).

Freiesleben, J., et al. (2020). "Machine learning and Design of Experiments: Alternative approaches or complementary methodologies for quality improvement?" Quality and Reliability Engineering International **36**(6): 1837-1848.

Gangi, A. F. (1978). Variation of whole and fractured porous rock permeability with confining pressure. International Journal of Rock Mechanics and Mining Sciences & Geomechanics Abstracts, Elsevier.

Gherabati, S. A., et al. (2018). "Assessment of hydrocarbon in place and recovery factors in the Eagle Ford Shale play." SPE Reservoir Evaluation & Engineering **21**(02): 291-306.

Gunst, R. F. and R. L. Mason (2009). "Fractional factorial design." Wiley Interdisciplinary Reviews: Computational Statistics **1**(2): 234-244.

Guo, X., et al. (2017). "Geological factors controlling shale gas enrichment and high production in Fuling shale gas field." Petroleum Exploration and Development **44**: 513-523.

Gupta, R., et al. (2008). History Matching Of Field Production Using Design Of Experiments, SPE.

Gurav, Y. S., et al. (2019). Application of Design of Experiments for Well Pattern Optimization in Umiat Oil Field: A Natural Petroleum Reserve of Alaska Case Study, SPE.

Hareland, G., et al. (1993). Hydraulic Fracturing Design Optimization, Society of Petroleum Engineers.

Hicks, C. R. (1964). "Fundamental concepts in the design of experiments."

Holditch, S. A. (2007). "Hydraulic fracturing: overview, trends, issues." Drilling Contractor **63**: 116-118.

Hughes, J. D. (2013). "A reality check on the shale revolution." Nature **494**(7437): 307-308.

Khuri, A. I. and S. Mukhopadhyay (2010). "Response surface methodology." Wiley Interdisciplinary Reviews: Computational Statistics **2**(2): 128-149.

Minitab, L. (2013). Minitab, State College Pennsylvania.

Olorode, O. M., et al. (2017). "Compositional reservoir-flow simulation for organic-rich gas shale." SPE journal **22**(06): 1963-1983.

Shah, J. J., et al. (2000). "Evaluation of Idea Generation Methods for Conceptual Design: Effectiveness Metrics and Design of Experiments." Journal of Mechanical Design **122**(4): 377-384.

Tang, X., et al. (2016). "Effect of Organic Matter and Maturity on Pore Size Distribution and Gas Storage Capacity in High-Mature to Post-Mature Shales." Energy & Fuels **30**(11): 8985-8996.

Wahid, Z. and N. Nadir (2013). "Improvement of one factor at a time through design of experiments." World Appl. Sci. J **21**: 56-61.

Warpinski, N. R., et al. (2009). "Stimulating unconventional reservoirs: maximizing network growth while optimizing fracture conductivity." Journal of Canadian Petroleum Technology **48**(10): 39-51.

Wasaki, A. and I. Y. Akkutlu (2015). "Permeability of organic-rich shale." SPE journal **20**(06): 1384-1396.